Separated-wavefield imaging using primary and multiple energy

Shaoping Lu[1], Dan N. Whitmore[1], Alejandro A. Valenciano[1], and Nizar Chemingui[1]

Abstract

Imaging with separated wavefields (SWIM) is an innovative depth-imaging technology that uses upgoing and downgoing wavefields at the surface to deliver high-resolution images of the subsurface. It takes advantage of the extended illumination provided by surface-multiple energy, and thus, it exploits data that the seismic industry historically has treated as unwanted noise. The fundamental concept behind SWIM is based on using each receiver as a "virtual" source, effectively expanding the surface coverage of the seismic experiment and enhancing the subsurface illumination, particularly for shallow reflectors. By effectively turning the streamer spread into a source (and receiver) array, the resulting equivalent survey has spatial sampling that is much improved and a richer distribution of offsets and azimuths. The improved spatial sampling enhances the angular illumination greatly at every image point. Therefore, SWIM produces densely sampled angle gathers that provide greater opportunities for velocity-model building and for improved interpretation of complex structures. Several issues need to be considered for proper imaging with SWIM: migration-imaging conditions, attenuation of cross talk, and acquisition design. The latter must be addressed to support proper sampling of both upgoing and downgoing wavefields used for imaging. A broad overview and examples of these subjects are presented. Applications to a deepwater wide-azimuth (WAZ) survey from the Gulf of Mexico and a shallow-water narrow-azimuth (NAZ) data set from offshore Malaysia demonstrate the enhanced areal illumination and improved imaging resolution from imaging using multiple-reflection energy.

Introduction

Wave-equation migration consists of numerically extrapolating source and receiver wavefields into the subsurface, where an imaging principle is applied (Claerbout, 1971). When imaging primary reflections, the source wavefield is initiated by a point source and propagated into the earth. The upgoing wavefield (P-UP), used as receiver wavefield at the surface, is obtained by deghosting the data. These surface recordings contain not only primary reflections but also multiple-scattered energy. When imaging primary reflections, the multiple-scattered waves are treated as noise that typically is attenuated in processing (e.g., surface-related multiple removal).

However, in the last decade, we have seen the use of multiple reflections for imaging as opposed to removing them as noise (Berkhout and Verschuur, 1994; Whitmore et al., 2010; Lu et al., 2015). In the case of dual-sensor streamer acquisition, the recorded data can be separated accurately into upgoing (P-UP) and downgoing (P-DWN) components (Carlson et al., 2007), both containing primaries and multiple-scattered energy. When imaging with separated wavefields, the P-DWN wavefield replaces the point-source wavefield used in imaging primary reflections. Effectively, this P-DWN wavefield is a virtual source array at each receiver position. To build an image, the P-DWN and P-UP wavefields are extrapolated into the earth, and the image is constructed by using an imaging principle (Figure 1a).

Methodology

Imaging with separate wavefields increases the surface coverage and subsurface illumination by turning each receiver into a virtual source. This principle is independent of the wave-equation propagation algorithm, which can be based on one-way or two-way solutions. In the examples shown here, imaging was achieved using a wave-equation-migration (WEM) process, in which a Fourier finite-difference (FFD) algorithm was used as a one-way wavefield-extrapolation operator. The FFD dispersion-relation approximation consists of three terms: a phase shift, a thin lens, and finite differences. The 3D finite-difference operator is implemented using multiway splitting that uses a different set of optimized coefficients along each splitting direction (Valenciano et al., 2009). This method is extremely efficient, particularly in tilted transversely isotropic (TTI) media, which makes it a good alternative for high-resolution imaging.

When shot-profile migration is applied, the imaging of multiples is a blending migration process in both spatial and temporal domains. Therefore, during the application of the chosen imaging condition, events generated by the correlation

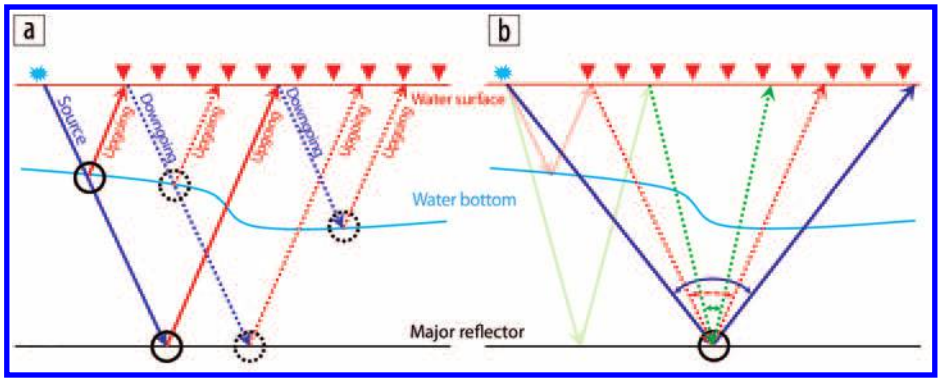

Figure 1. (a) Schematic diagram for trajectories of primary wavefield (solid lines) and multiple wavefield (dashed lines). Images from multiple reflection signals (dashed circles) illuminate greater subsurface extent than images from primary reflection signals (solid circles). (b) At a subsurface reflector (solid circle), the primary wavefield contains a single reflection angle (blue), and the multiple wavefield contains more than one reflection angle (red and green).

[1]Petroleum Geo-Services.

http://dx.doi.org/10.1190/tle34070770.1.

of unrelated P-UP and P-DWN wavefields appear as cross talk in the images. The cross talk can be reduced partially in the stacking process by using an acquisition with large data extent in space and time (i.e., wide acquisition spread and long recording length). Here, we discuss the use of an imaging condition that can assist in the reduction of cross talk, but we note that more advanced inversion methods might be needed to remove it fully.

The reflection coefficient, in shot-record, wave-equation migration, can be estimated as the deconvolution of the receiver by the source wavefield (Claerbout, 1971). However, for practical reasons and primarily for stability, the imaging condition usually is implemented as crosscorrelation of the receiver and the source wavefields as

$$I(\bar{x}) = \sum_{\bar{x}_s} \sum_{\omega} P_{\text{up}}(\bar{x}_s, \bar{x}, \omega) P^*_{\text{down}}(\bar{x}_s, \bar{x}, \omega), \quad (1)$$

in which P_{up} and P_{down} represent the P-UP and P-DWN wavefields, respectively, at an image point $\bar{x}$. The P-UP and P-DWN wavefields are initiated using a common source $\bar{x}$ and are represented in the frequency domain ω. Although this crosscorrelation imaging condition (equation 1) is stable and is correct kinematically, it cannot produce true relative amplitudes and is susceptible to cross talk when imaging with multiples. In contrast, the stabilized, deconvolution imaging condition (Guitton et al., 2007)

$$R(\bar{x}) = \sum_{\bar{x}_s} \sum_{\omega} \frac{P_{\text{up}}(\bar{x}_s, \bar{x}, \omega) P^*_{\text{down}}(\bar{x}_s, \bar{x}, \omega)}{\left\langle P_{\text{down}}(\bar{x}_s, \bar{x}, \omega) P^*_{\text{down}}(\bar{x}_s, \bar{x}, \omega) \right\rangle_{\bar{x}} + \varepsilon(\bar{x}_s, \bar{x}, \omega)} \quad (2)$$

creates an estimate of the subsurface reflectivity $R(\bar{x})$ and provides a reduction in cross talk. The deconvolution imaging condition includes the denominator that is smoothed in the space domain $\langle\ \rangle_{\bar{x}}$ and a stabilization term $\varepsilon(\bar{x}_s, \bar{x}, \omega)$. The effect of the deconvolution imaging condition is demonstrated when applied to an SEG Advanced Modeling (SEAM) synthetic example. In Figure 2, we compare a section of the images from multiples generated using either the crosscorrelation (Figure 2a) or deconvolution (Figure 2b) imaging condition. The deconvolution imaging condition produces amplitudes closer to the reflection coefficient, and overall, an image with higher signal-to-noise ratio (S/N).

Equation 2 can be generalized to the prestack image domain by extending the image to create subsurface prestack offset gathers $I(\bar{x}, \bar{h})$. They are computed by deconvolving the shifted subsurface P-UP and P-DWN wavefields as

$$I(\bar{x}, \bar{h}) = \sum_{\bar{x}_s} \sum_{\omega} \frac{P_{\text{up}}(\bar{x}_s, \bar{x}, \omega, \bar{x} + \bar{h}) P^*_{\text{down}}(\bar{x}_s, \bar{x}, \omega, \bar{x} - \bar{h})}{\left\langle P_{\text{down}}(\bar{x}_s, \bar{x}, \omega, \bar{x} - \bar{h}) P^*_{\text{down}}(\bar{x}_s, \bar{x}, \omega, \bar{x} - \bar{h}) \right\rangle_{\bar{x}} + \varepsilon(\bar{x}_s, \bar{x}, \omega)}, \quad (3)$$

in which $\bar{h}$ is the source-receiver half offset. The resulting subsurface offset images can be transformed to the angle domain through a radial-trace transformation (Rickett and Sava, 2002).

Although some cross talk can be reduced by applying the deconvolution imaging condition during migration, the remaining cross talk can be predicted and attenuated after migration in the image space. Cross talk is created from the correlation between unrelated multiples and primaries. It can be categorized into causal or anticausal components, according to the position and time they appear in the image compared with their corresponding true reflection locations. Most causal and anticausal components can be predicted. Figure 3a displays the raw SWIM image, which is contaminated by both anticausal (red oval) and causal (blue arrow) cross talk. The predicted cross talk can be seen in Figures 3c and 3d. Figure 3b shows the SWIM image after postmigration cross-talk attenuation.

Advantages of separated-wavefield imaging

The basic principle behind SWIM is the use of each receiver as a "virtual" source, effectively expanding the surface coverage of the seismic experiment and enhancing the subsurface illumination. By turning the streamer spread into an areal source (and receiver) array, the resulting equivalent survey has improved spatial sampling and a richer distribution of offsets and azimuths. This is illustrated by using single-arrival rays in Figure 1a. Within a one-shot physical experiment, multiples can travel through a broader subsurface region than primaries can. In shot-profile migration, the lateral extent of the illumination zone is approximated by the source-receiver midpoint. When imaging with primaries, the illumination area is concentrated toward the common source location. When imaging using multiples, the subsurface region covered by the receivers in the surface is illuminated.

Imaging using multiple-reflection energy improves the resolution of each

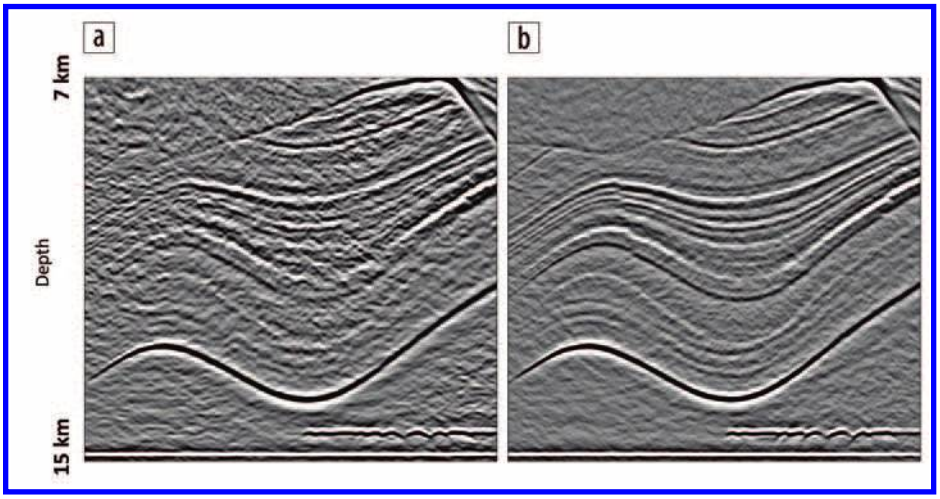

Figure 2. Inline images for SWIM using (a) crosscorrelation imaging condition and (b) deconvolution imaging condition. The deconvolution imaging condition suppresses cross talk and provides an image with higher signal-to-noise ratio.

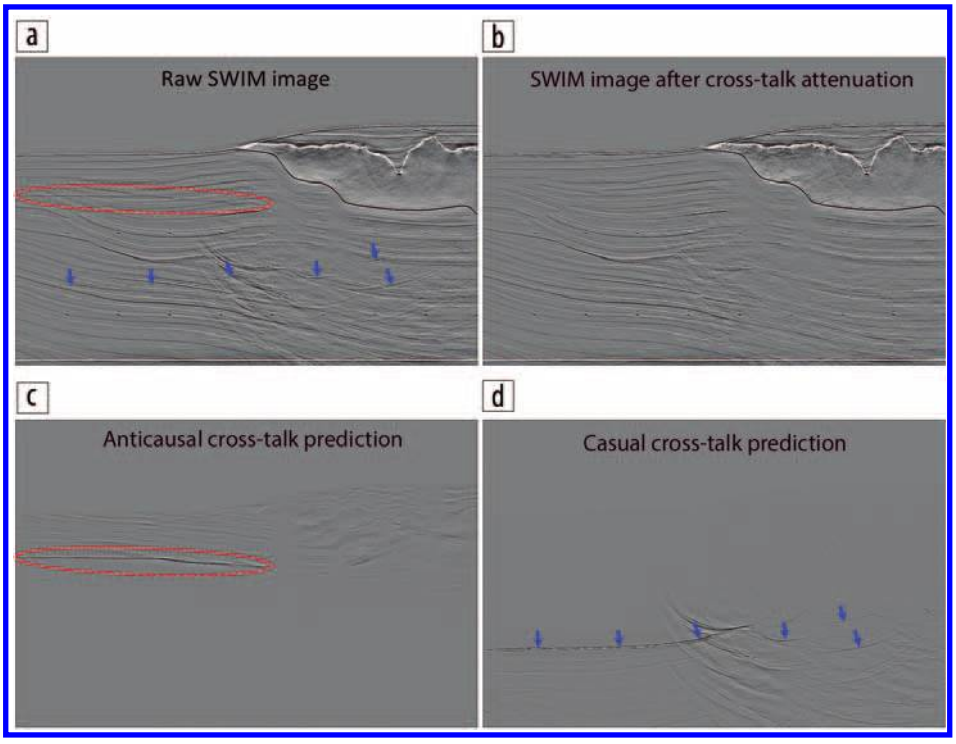

Figure 3. Cross-talk prediction and attenuation for SWIM. (a) Raw SWIM image, (b) SWIM image after cross-talk attenuation, (c) anticausal cross-talk prediction, and (d) causal cross-talk prediction.

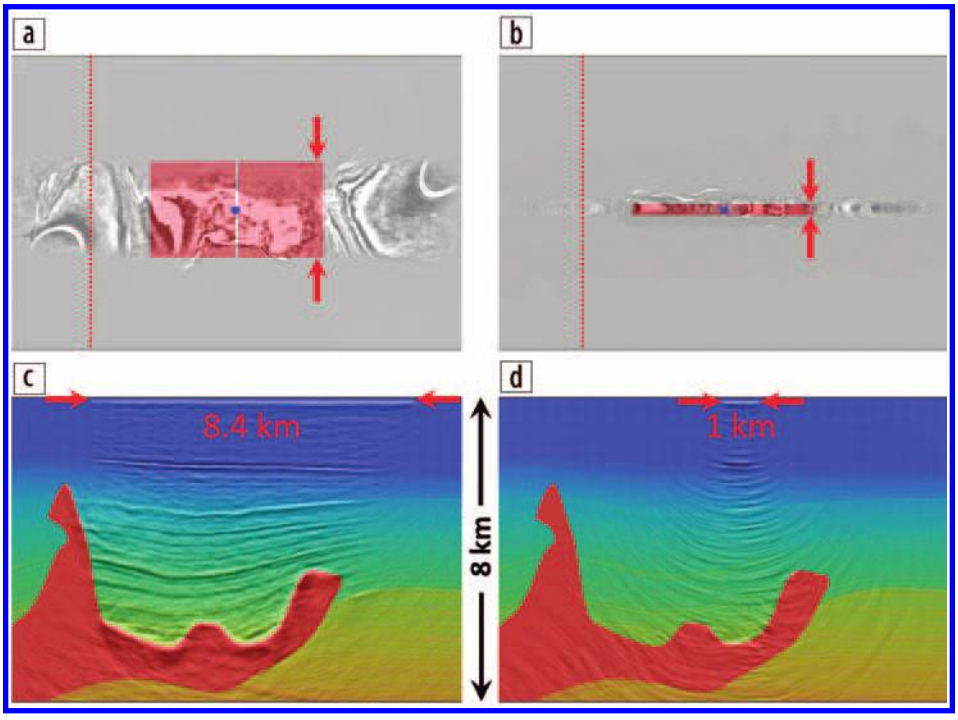

Figure 4. Images of multiples using one sail line from the SEAM model: (a) and (c) WAZ; (b) and (d) NAZ. On top of the 2-km depth slices in parts (a) and (b), pink areas indicate shooting geometries (of one shot). The WAZ shot has 14-km inline and 8.4-km crossline split-spread acquisition offset. The NAZ shot has 16-km inline and 1-km crossline split-spread acquisition offset. Panels (c) and (d) display crossline-direction depth images on top of the velocity model. Dashed red lines in (a) and (b) indicate the location from which the crossline images (c) and (d) are extracted. Red arrows in (a) and (b) indicate the streamer offset at the crossline direction, which is consistent with the strong coherent events in the crossline direction at the sea surface, shown by red arrows in (c) and (d).

image point by using many reflection angles. From a single-shot point of view, Figure 1b shows how the plurality of "virtual" sources from the multiples can illuminate the same reflection point from more than one angle, although the primaries can illuminate the same reflection point only once. When considering a subsurface reflection point, the angular illumination depends on the source density. Imaging using multiples turns each receiver array into a virtual source, so the equivalent source density of migration is equal to the receiver density. In a typical towed-streamer marine seismic acquisition, receivers are sampled more densely than sources along a line, and the cable spacing of a multistreamer survey is smaller than the sail-line spacing. As a result, the virtual sources illuminate the reflectors from denser reflection angles, improving the resolution of each image point.

Acquisition factors affecting imaging with separated wavefields

In SWIM, the separated P-DWN and P-UP wavefields are used as source and receiver wavefields, respectively, and must be sampled and recorded properly during acquisition. The streamer coverage, receiver density, source-receiver distribution geometry, acquisition shooting direction, target depth, and subsurface dip all are controlling factors in the effectiveness of SWIM.

The maximum offset determines both the P-DWN and P-UP wavefield coverage. Broader and denser streamer coverage produces more complete source-and-receiver wavefields and improves SWIM image quality. Figure 4 displays the SWIM results from a deepwater wide-azimuth survey and a shallow-water narrow-azimuth survey from one sail line of the SEAM synthetics. For the depth slices (Figures 4a and 4b) and crossline direction images (Figures 4c and 4d), the comparison shows that WAZ generates much broader subsurface illumination than NAZ does.

The image quality from SWIM also is affected by the shooting

direction and source-receiver distribution geometry. Single-ended streamer acquisition causes a directional bias in the ability to image multiples. For example, if a multiple generator is relatively flat, the direction of the P-DWN wavefield is directed mostly toward the cable tails. Therefore, the multiples can image small dips, shallow dips, and downdips (Figures 5c and 5d). On the other hand, the multiples have limited ability to illuminate updips, especially when the target is deep relative to the longest offset (Figures 5c and 5e). Antiparallel shooting can image the dipping target from the opposite shooting direction (Figure 5d). The split-spread shot gather can use the downgoing and upgoing wavefields recorded at different sides of the shot location and can image updips and downdips from one shot (Figure 5f). In towed-streamer acquisition, split-spread shot gathers can be generated by using head-tail shooting.

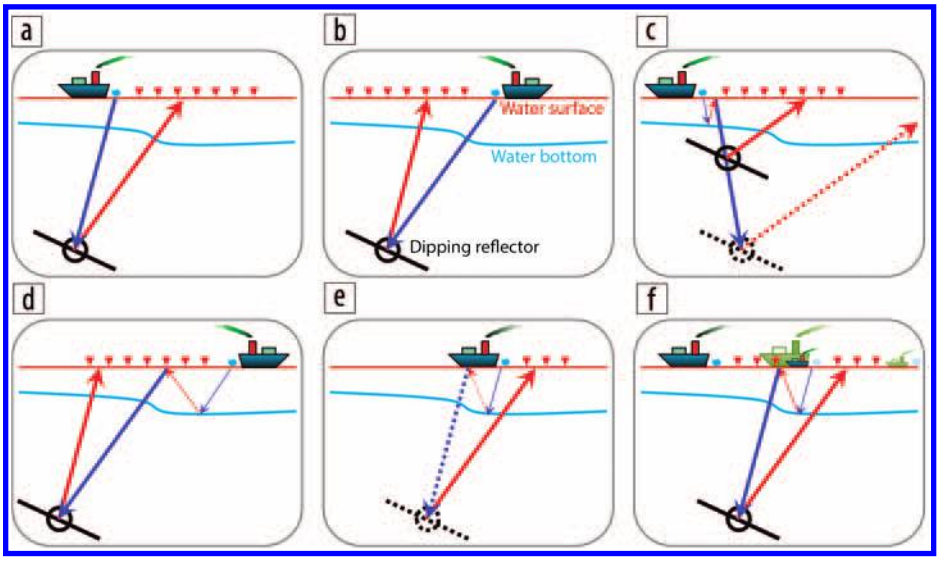

Figure 5. Schematic diagrams demonstrate the effects of acquisition geometry on imaging of multiples. Arrows display wavefields — blue is downgoing, red is upgoing, solid is recorded, and dashed is misrecorded. Solid circles are imaging construction points; dashed circles are nonimaging construction points. (a) and (b) show raypaths of primary imaging, in which updip and downdip are imaged by equivalent raypaths from either shooting direction. (c) and (e) show that imaging of multiples has limitations to image updips. In (c), the updip could be imaged by multiples when the target is shallow; however, deeper updip cannot be imaged because either source wavefield (downgoing in [e]) or receiver wavefield (upgoing in [c]) is not recorded. (d) shows that antiparallel shooting can image the dipping target as the downdip from the opposite shooting direction. (f) shows that the split-spread shot can generate even more illumination by using downgoing and upgoing wavefields recorded from opposite sides of the shot location.

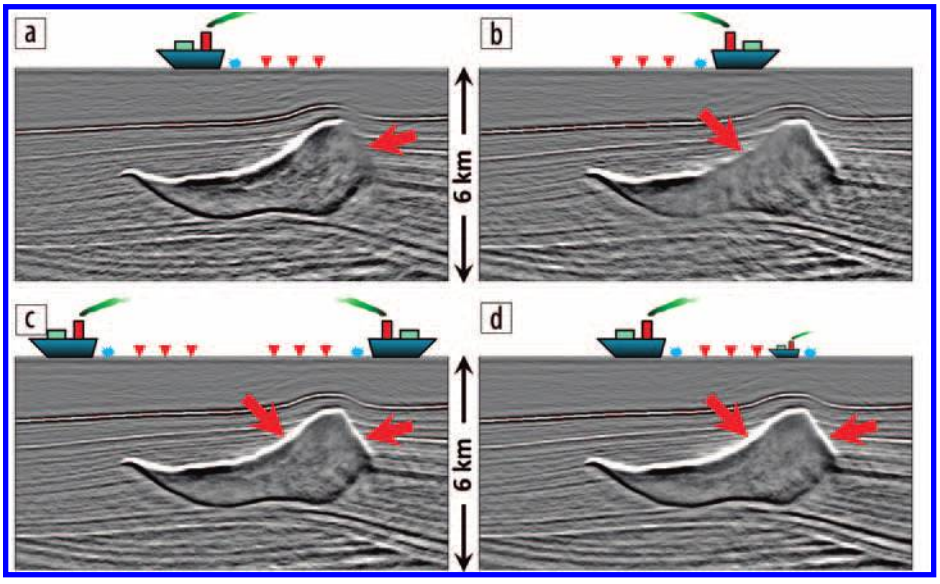

Figure 6. Inline-direction images of multiples from using different shooting geometries (WAZ): (a) and (b) single-direction shooting, (c) antiparallel shooting, and (d) split-spread shooting generated from head-tail shooting.

To demonstrate the biased shooting-direction effects in SWIM, results from 3D SEAM synthetics are used for discussion. Figure 6 shows images from multiples using different shooting geometries. Single-direction shooting (Figures 6a and 6b) has limitations in imaging the updips because either the P-DWN or P-UP wavefield is not recorded. Antiparallel shooting (Figure 6c) is a direct summation of the single-direction imaging results shown in Figures 6a and 6b; therefore, the dips of both directions are imaged. Compared with Figure 6c, split-spread shooting (Figure 6d) generates the best result by using the extra raypaths in Figure 5f.

Wide-azimuth field data application

The effectiveness of imaging with multiples depends strongly on the overall streamer coverage, receiver density, and source-receiver geometry. The more free-surface, multiple-reflection information that can be collected by the chosen receiver-array geometry, the more the final image potentially can be improved. For this reason, SWIM technology is particularly advantageous in improving subsurface illumination and imaging resolution when used with WAZ survey geometries.

To illustrate this, we have applied the tilted transversely isotropic SWIM technique to a WAZ data set acquired in the deepwater Gulf of Mexico. Results from this example demonstrate the improved imaging resolution, especially for complex structures of salt boundaries. Figures 7a and 7b show a comparison of depth slices from imaging of primaries only and imaging with multiples at 3 km below the sea surface. The results illustrate much improved resolution from imaging using multiples — a better lateral definition of the rugose top-salt geometry. The close-up images in Figures 7a and 7b confirm that multiples

produce more continuous and clearer salt-boundary images than primaries alone.

The significantly improved illumination and resolution provided by SWIM can be accessed best in prestack domain by looking at angle gathers. Subsurface illumination using primaries is limited by the shot density, which is controlled by the shot and sail-line spacing (typically several hundred meters). Sampling of free-surface multiples used in SWIM is determined by receiver and cable spacing, which is typically much denser than shot and sail-line spacing. Therefore, imaging with multiples generates more finely sampled angle gathers, especially in the crossline direction. The angle gathers centered on the water bottom, sediment, and top salt can be seen in Figures 7c through 7f. In the plots, the angle gathers are displayed in inline (zero-degree azimuth) and crossline (90° azimuth) directions, with maximum angles ranging from –70° to +70°. Figure 7d shows zero-degree-azimuth angle gathers from SWIM, which are sampled much more finely than the gathers from imaging with primaries only

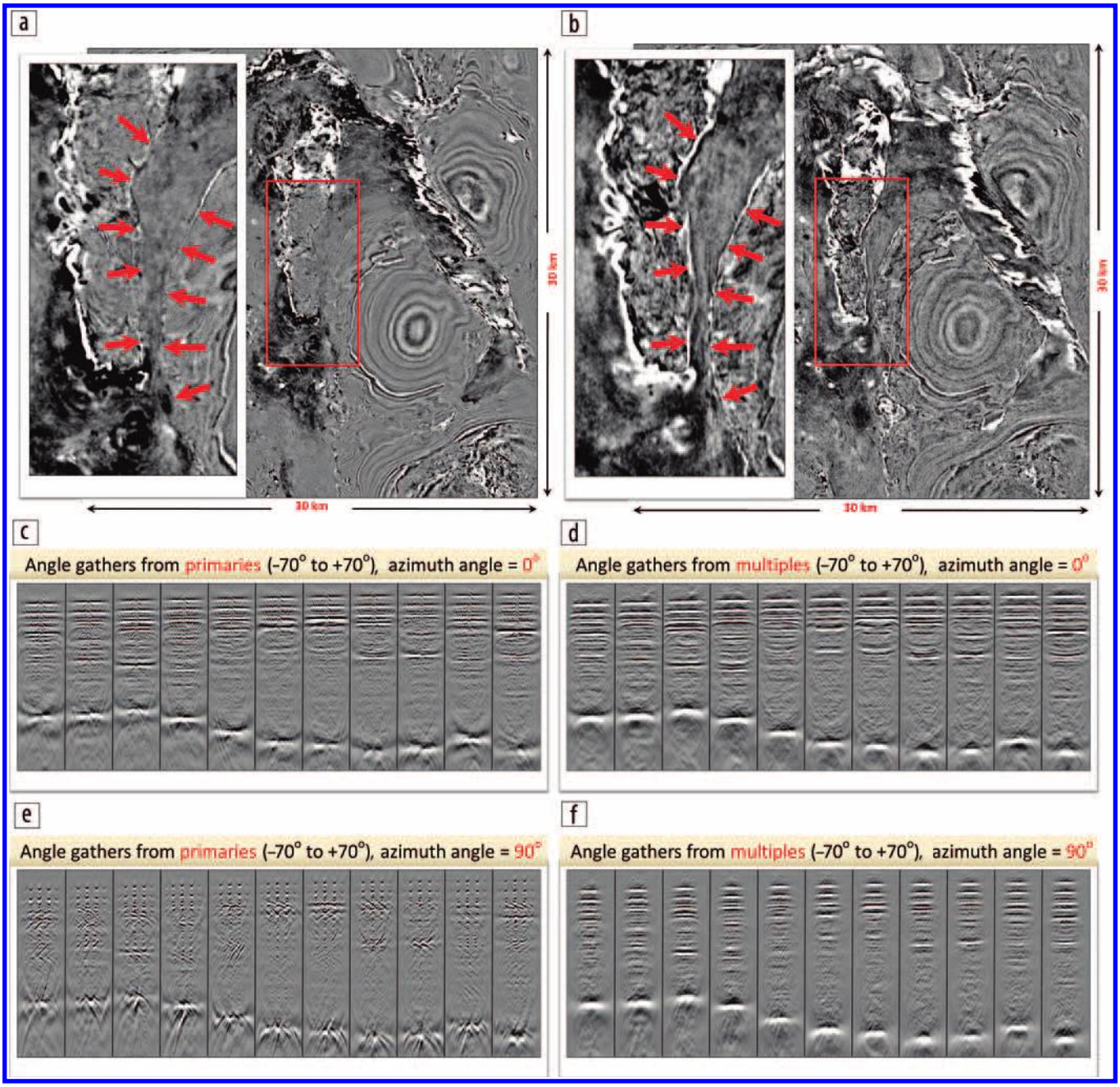

Figure 7. Depth slices (3000 m below the sea surface) from (a) imaging of primaries and (b) SWIM. Separated-wavefield imaging improves illumination of complex top-salt structures (indicated using arrows inside the red boxes). (c) Angle gathers from primaries only (inline direction). (d) Angle gathers from multiples using SWIM (inline direction). (e) Angle gathers from primaries in the crossline (90°-azimuth) direction, with very few reflection angles imaged. (f) Densely populated angle gathers from SWIM (crossline direction) that are easier to interpret. The improved illumination and resolution provided by SWIM can be accessed best in prestack domain by looking at angle gathers. Poor angular illumination in gathers that use primaries only arises from coarse crossline shot sampling. Gathers from SWIM, however, are sampled finely in both inline and crossline directions.

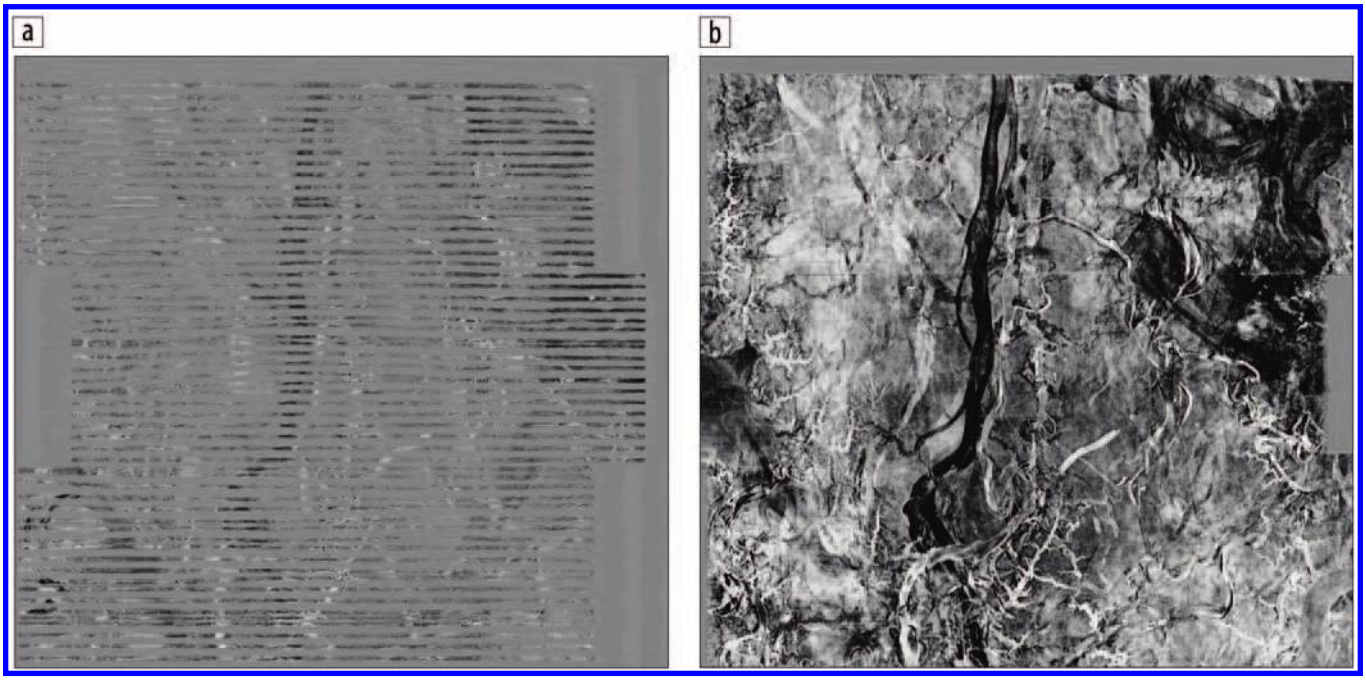

Figure 8. Depth slices at 105 m below sea surface in an area with 70-m water depth from (a) a primary-only image and (b) SWIM. The image from SWIM not only provides a larger subsurface coverage at this depth, but it also includes details that are not present in the primaries-only image.

(Figure 7c). Moreover, in the 90°-azimuth direction, only a few reflection angles are imaged (Figure 7e). Figure 7f shows the densely populated angle gathers from SWIM that are easier to interpret. The densely populated angle-domain images greatly improve imaging resolution in the stack domain.

Narrow-azimuth field data application

Although imaging using multiples benefits from the large streamer array used in WAZ survey geometries, it also improves the areal illumination and resolution of shallow-subsurface targets when applied to NAZ data. The acquisition footprint and poor near-surface image resolution present ongoing challenges, particularly in shallow-water environments when only primaries are used for imaging. In imaging using primaries only, the acquisition footprint is caused by large shot spacing in the crossline direction. By using each receiver array as a pseudosource, SWIM has much denser shot in both inline and crossline directions and can expand the illumination area and mitigate the sail-line footprint. The large and sparse angular illumination from imaging of primaries creates lower-resolution images, especially for shallow structures. By imaging denser and relatively smaller reflection angles, SWIM generates higher-resolution images.

To improve the image resolution, high-density 3D (HD3D) acquisition-survey geometries can be designed, comprising denser sail-line spacing and richer near-offset information. However, this increases the cost of both acquisition and data processing. As discussed above, free-surface multiples provide a significantly wider and denser sampling of shallow reflectors than is possible with primary arrivals. Therefore, SWIM provides a possible low-cost alternative to high-density acquisition geometries in shallow-water environments.

We illustrate the near-surface-image improvements by applying imaging multiples to a NAZ data set from offshore Malaysia. In a 25-km × 23.4-km testing area, 49 consecutive sail lines of dual-sensor streamer data are imaged using P-UP and P-DWN wavefield estimates. Figure 8 shows depth sections at 105 m below the sea surface for the primary-only image (Figure 8a) and the SWIM image (Figure 8b). Significant gaps are visible in the primary-only image of the shallow overburden, caused by the required mutes to eliminate refracted energy arrivals. In contrast, the SWIM images have a complete and high-resolution near-surface image (Figure 8b), which provides a shallow-channel image of excellent clarity and structural detail.

Conclusions

SWIM uses upgoing and downgoing wavefields (both containing primaries and multiple-scattered energy) in depth migration to produce high-resolution images of the subsurface. In the case of dual-sensor streamer acquisition, the recorded data can be separated accurately into P-UP and P-DWN components. These components are used as source and receiver wavefields, respectively, in shot-profile wave-equation migration and must be sampled and recorded properly during acquisition. Streamer coverage, receiver density, source-receiver distribution geometry, acquisition shooting direction, target depth, and subsurface dip are all controlling factors in the quality of the image from SWIM.

In SWIM, the P-DWN wavefield is used as a virtual areal source, resulting in images with increased angular illumination. As a result, the use of multiples improves the extent of the subsurface image and its resolution. Significant near-surface image improvements are observed for both wide-azimuth and narrow-azimuth geometries.

The process of using P-DWN wavefield as a virtual areal source can create cross talk. This cross talk can be reduced by using a deconvolution imaging condition during migration. The remaining cross talk can be predicted in the image domain and can be attenuated using postmigration processes.

Ultimately, the most complete images come from the combination of primaries and multiples. Many emerging technical advances in the industry are based on inversion methods, which attempt to invert the total wavefield (primaries, surface-related multiples, and internal multiples). This requires not only advanced modeling and inversion methods but also an understanding of how acquisition affects the quality of the inversion results. This article demonstrates the importance of using more of the total wavefield for imaging and the necessity of understanding the effects of acquisition on image quality and completeness.

Multiples can provide additional value to imaging in marine-streamer acquisition, but there are other scenarios in which multiples add value. These include ocean-bottom seismic acquisition or 3D vertical seismic profiles (VSP), in which reciprocal imaging of receiver gathers can be used. TLE

Acknowledgments

We thank our colleagues Jack Kinkead and Hui Le Gleut for their help and support in the work presented here. We acknowledge SEG for providing the original SEAM model and data. We thank Lundin Malaysia BV and PETRONAS Carigali Sdn. Bhd. (Lundin Malaysia BV's partners in PM307) for their support of the Malaysia NAZ imaging project and PGS MultiClient for their support in the Gulf of Mexico WAZ imaging project. We thank PGS for its support and for permission to publish this work.

Corresponding author: Shaoping.Lu@pgs.com

References

Berkhout, A. J., and D. J. Verschuur, 1994, Multiple technology: Part 2, migration of multiple reflections: 64th Annual International Meeting, SEG, Expanded Abstracts, **23**, 1497–1500, http://dx.doi.org/10.1190/1.1822821.

Carlson, D., A. Long, W. Söllner, H. Tabti, R. Tenghamn, and N. Lunde, 2007, Increased resolution and penetration from a towed dual-sensor streamer: First Break, **25**, 71–77.

Claerbout, J. F., 1971, Toward a unified theory of reflector mapping: Geophysics, **36,** 467–481, http://dx.doi.org/10.1190/1.1440185.

Guitton, A., A. Valenciano, D. Bevc, and J. Claerbout, 2007, Smoothing image condition for shot-profile migration: Geophysics, **72**, no. 3, S149–S154, http://dx.doi.org/10.1190/1.2712113.

Lu, S., A. A. Valenciano, N. Chemingui, and D. B. Lecerf, 2015, Separated wavefield imaging of ocean bottom seismic (OBS) data: 77th Conference and Exhibition, EAGE, Extended Abstract, http://dx.doi.org/10.3997/2214-4609.201412943.

Rickett, J., and P. Sava, 2002, Offset and angle-domain common image-point gathers for shot-profile migration: Geophysics, **67**, 883–889, http://dx.doi.org/10.1190/1.1484531.

Valenciano, A. A., C. C. Cheng, N. Chemingui, and S. Brandsberg-Dahl, 2009, Fourier finite-difference migration for 3D TTI media: 71st Conference and Exhibition, EAGE, Extended Abstracts, P065.

Whitmore, N. D., A. Valenciano, W. Söllner, and S. Lu, 2010, Imaging of primaries and multiples using a dual-sensor towed streamer: 80th Annual International Meeting, SEG, Expanded Abstracts, 3187–3192, http://dx.doi.org/10.1190/1.3513508.